Available online at www.sciencedirect.com
SCIENCE DIRECT®
C. R. Biologies 328 (2005) 223–234
COMPTES RENDUS BIOLOGIES
http://france.elsevier.com/direct/CRASS3/

Neurosciences

# A chimera encoding the fusion of an acetylcholine-binding protein to an ion channel is stabilized in a state close to the desensitized form of ligand-gated ion channels

Thomas Grutter [a,*], Lia Prado de Carvalho [a], Virginie Dufresne [a], Antoine Taly [a], Markus Fischer [b], Jean-Pierre Changeux [a]

[a] *Récepteurs et Cognition, URA CNRS 2182, Institut Pasteur, 25, rue du Docteur-Roux, 75724 Paris cedex 15, France*
[b] *Lehrstuhl für Organische Chemie und Biochemie der Technischen Universität München, Germany*

Received 24 September 2004; accepted 17 November 2004

Presented by Jean-Pierre Changeux

**Abstract**

To understand the mechanism of allosteric coupling between the ligand-binding domain and the ion channel of the Cys-loop ligand-gated ion channels (LGICs), we fused the soluble acetylcholine-binding protein (AChBP), which lacks an ion channel, to either the cationic serotonin type-3A ion channel ($5HT_{3A}$) or the anionic glycine ion channel. Both linear chimeras expressed in HEK-293 cells display high affinity for the nicotinic agonist epibatidine ($K_D = 0.2$–$0.5$ nM), but are not targeted to the cell surface. Only after substituting a ring of three loops located at the putative membrane side of the AChBP three-dimensional structure by the homologous residues of $5HT_{3A}$, the resulting chimera AChBP(ring)/$5HT_{3A}$ (*i*) still displayed on intact cells an apparent high affinity for epibatidine, yet with a fourfold decrease ($K_D = 2.1$ nM), (*ii*) displayed a high proportion of low affinity sites ($11 \pm 7$ μM) for the resting state stabilizing competitive antagonist α-bungarotoxin and (*iii*) was successfully targeted to the cell surface, as seen by immunofluorescence labelling. The AChBP(ring)/$5HT_{3A}$ chimera forms a pentameric structure, as revealed by sucrose gradient sedimentation. However, no whole-cell patch-clamp currents were detectable. Interestingly, binding assays with membrane fragments prepared from cells expressing AChBP(ring)/$5HT_{3A}$ showed a decrease in the apparent affinity for the agonists nicotine and epibatidine (5-fold), concomitant with an increase in the proportion of high-affinity sites ($48 \pm 1$ nM) for α-bungarotoxin. These results indicate that fusion of AChBP to an ion channel forms a pentameric receptor exposed to the cell surface and able to convert between discrete allosteric states, but stabilized in a high affinity state for epibatidine that likely corresponds to a desensitized form of LGICs. These artificial chimeras might offer a useful system to investigate signal transduction in LGICs. ***To cite this article: T. Grutter et al., C. R. Biologies 328 (2005).***
© 2004 Académie des sciences. Published by Elsevier SAS. All rights reserved.

* Corresponding author.
*E-mail addresses:* grutter@pasteur.fr (T. Grutter), changeux@pasteur.fr (J.-P. Changeux).

1631-0691/$ – see front matter © 2004 Académie des sciences. Published by Elsevier SAS. All rights reserved.
doi:10.1016/j.crvi.2004.11.004

**Résumé**

**Une chimère formée par la fusion d'une protéine liant l'acétylcholine à un canal ionique est stabilisée dans un état proche de la forme désensibilisée des récepteurs-canaux activables par un ligand.** Afin de comprendre les mécanismes de couplage entre le domaine de liaison de l'acétylcholine (ACh) et son canal ionique, nous avons fusionné la protéine soluble liant l'ACh (AChBP) naturellement dépourvue de canal, soit à un canal cationique sérotoninergique ($5HT_{3A}$), soit à un canal anionique glycinergique. Ces chimères AChBP/$5HT_3$ et AChBP/Gly possèdent une haute affinité pour l'agoniste épibatidine similaire à l'affinité pour l'AChBP soluble, mais ne sont pas adressées à la membrane plasmique. En revanche, en substituant trois boucles localisées sur la face membranaire hypothétique de l'AChBP par les résidus homologues « sérotonine » dans la chimère AChBP/$5HT_3$, la chimère correspondante AChBP(ring)/$5HT_3$ (*i*) manifeste encore une haute affinité pour l'épibatidine, avec toutefois une légère baisse d'affinité ($K_D = 2.1$ nM), (*ii*) présente une forte proportion de sites de basse affinité pour l'$\alpha$-bungarotoxine, qui bloque de manière compétitive le récepteur sous l'état de repos, et (*iii*) est adressée à la surface de la cellule. Cette chimère forme un pentamère mis en évidence par des expériences de centrifugation sur gradient de saccharose, mais aucun courant n'est détecté par électrophysiologie en condition cellule entière. Cependant, en préparant des membranes à partir de cellules transfectées par la chimère AChBP(ring)/$5HT_3$, nous décrivons une perte d'affinité pour les agonistes (5 fois), concomitante à une augmentation des sites de haute affinité pour l'$\alpha$-bungarotoxine. Nous en concluons que la chimère forme un pentamère de surface capable d'effectuer des transitions allostériques, mais qu'elle est bloquée dans un état de haute affinité pour l'épibatidine, qui correspond probablement à la forme désensibilisée du récepteur. ***Pour citer cet article : T. Grutter et al., C. R. Biologies 328 (2005).***

© 2004 Académie des sciences. Published by Elsevier SAS. All rights reserved.

*Keywords:* AChBP; Acetylcholine; Nicotinic; Receptor; Pentameric ligand-gated ion channel; Allosteric transitions

*Mots-clés :* AChBP ; Acétylcholine ; Nicotinique ; Récepteur ; Canal ionique liée à un ligand pentamère ; Transitions allostériques

## 1. Introduction

Ligand-gated ion channels (LGICs) of the Cys-loop super-family mediate fast neurotransmission. These receptors are composed of three domains: an extracellular domain composing the ligand-binding pocket, a transmembrane ion channel domain, and an intracellular domain that carries phosphorylation sites [1,2]. Upon agonist application, these receptors undergo a rapid conformational transition from a resting basal state (B state) to an open-channel state (A state). Prolonged application of the agonist promotes the stabilization of the receptor in a refractory high-affinity desensitized state (D state). This kinetic scheme is accounted for by an extended concerted allosteric model [3]. Early studies with chimeras between members of the LGICs super-family revealed that functional chimeric constructs can be obtained between $\alpha$7 nicotinic acetylcholine (ACh) receptor (nAChR) and serotonin type-3A ($5HT_{3A}$) receptor, underlying the functional autonomy of the ligand-binding and channel domains [4].

In the absence of X-ray data for the whole receptor, structures of individual domains are now available to mean atomic resolution [5,6]. First, the structure of an acetylcholine-binding protein (AChBP) from the fresh water snail *Lymnaea stagnalis*, homologous to the extracellular domain of nicotinic receptors [7], has been reported at 2.7 Å by X-ray crystallography [5]. The structure revealed a $\beta$-sandwich core composed of two twisted $\beta$-sheets. This pentameric protein, which naturally lacks an ion channel, offers an exceptional template for the modelling of the ligand-binding domain for the nicotinic receptor and all members of the LGIC [8–10] and led to the resolution at the atomic level of the complex of nicotine with its specific binding site [11]. Second, electron-microscopy (EM) pictures of *Torpedo marmorata* receptor have resolved at 4 Å an all $\alpha$-helix folds of the transmembrane domain [6]. Though the recent EM pictures still lack atomic resolution, the data offer the possibility to build a 3D model of the entire receptor: a synaptic $\beta$-sandwich ligand-binding module coupled to a four transmembrane $\alpha$-helices ion channel (Taly et al., manuscript submitted).

Cross-linking studies with the GABA-A receptor pinpointed a set of loops that interact between the two domains [12]. Asp-149 residue of the highly con-

served Cys-loop (or loop 7 in nomenclature from [5]) is at about 5 Å from Lys-279 located in C-terminal end of helix M2 in the $\alpha$1-subunit in GABA-A receptor [12]. The homologous residue in $\beta$2-subunit Asp-146 was found to interact with Lys-215 in the pre-M1 segment [13]. Similarly, Asp-57 of loop 2 is also close to Lys-279 in the M2 helix in the $\beta$-subunit in GABA. These studies define at least loops 2 and 7 located at the bottom side of the extracellular domain that link the synaptic and ion channel domains. However, how the two domains interact in the course of allosteric transitions remains unclear.

In this paper, we fused AChBP either with the ion channel and intracellular domains of the cationic serotonin type-3A ($5HT_{3A}$) receptor or with the anionic glycine receptor. First, AChBP was chosen because its atomic structure is known [5]; second AChBP forms an homopentameric assembly as do $5HT_{3A}$ and glycine receptors; and finally AChBP has most likely evolved without the constraint of an ion channel, and may (or not) have lost the possibility to undergo allosteric transitions. Here, we show that AChBP linearly fused with an ion channel forms high-affinity sites similar to that of the water-soluble form of AChBP; however, the fused protein is not targeted to the cell surface. Yet, after substituting a ring of three loops located at the putative membrane side of the three-dimensional structure of AChBP (loop 2, 7 and 9) with the homologous residues of $5HT_{3A}$, the resulting chimera AChBP(ring)/$5HT_{3A}$ is successfully targeted to the cell surface, as seen by immunofluorescence and assembles as a pentamer, as observed on sucrose gradient sedimentation. However, this chimera displays a high proportion of low-affinity sites (micromolar range) for the resting state stabilizing competitive antagonist $\alpha$-bungarotoxin ($\alpha$-BgTx) and does not give significant ACh-gated currents in whole-cell patch-clamp experiments. Interestingly, in vitro binding assays with membrane fragments prepared from cells expressing AChBP(ring)/$5HT_{3A}$ chimera show a decrease in the apparent affinity for agonist concomitantly with an increase of the proportion of high-affinity sites (low nanomolar range) for $\alpha$-BgTx. These results demonstrate that when fused into a ring chimera with the $5HT_{3A}$ channel, AChBP is capable of making allosteric transitions when expressed in HEK-293 cells, but remains stabilized in the high-affinity state for epibatidine, which likely corresponds to a desensitized form in LGICs. We conclude that part of the AChBP structure has retained during evolution some structural elements that allow allosteric transitions.

## 2. Materials and methods

### 2.1. cDNA constructs and site-directed mutagenesis

Synthetic genes for the *Lymnaea stagnalis* AChBP and *Gallus gallus* $\alpha$7 extracellular domain were engineered by multiple PCR amplifications of synthetic oligonucleotides containing silent restriction sites at 50 base pair intervals respecting mammalian-codon frequency usage. cDNAs encoding AChBP and the $\alpha$7 extracellular domain were subcloned into the plasmid pMT3 and both contained in 5′ the peptide signal sequence of $\alpha$7 nAChR subunit. The pore domain of the $5HT_{3A}$ or the glycine receptor was joined to AChBP or to $\alpha$7 extracellular domain with a mutagenically-introduced *Sal1* site, thus yielding a fusion site after Arg-202 of AChBP. The ring chimera was obtained by PCR amplification of AChBP sequence with primers 5′-TTCATCAACATCCTCGAGGTGGATGAGAAGAACCAGGTTCTGGACGTTGTCTTTTGGCAGCAGACGACATGG and 5′-CTTTACATGCCATCGATCCGC CAACGTTTCTCCTGTAGTCTAGACATCTACAACTTCCCCTTTGATGTGCAGAACTGTCGTATCAAAATTGGCAGC and 5′-CGACAGAAAATAGTGACGATTCTGAATACTTCATAAATCAGGGCGAGTGGGAGATCTTGGATGTCAC that contained the corresponding $5HT_{3A}$ sequences. The same procedure was followed with the $\alpha$7 extracellular domain for engineering the corresponding ring. PCR fragments were then subcloned into pMT3 into the silent restriction sites. All constructs except AChBP were tagged at the C-terminal end with the human Influenza hemagglutinin (HA) epitope (YPYDVPDYA). The nine HA epitope codons (5′-TACCCATACGACGTCCCAGACTACGCT) and a stop codon were inserted by PCR after the last codon of the 3′ translated region of the chimeric cDNAs. All constructs were verified by restriction maps and sequencing.

### 2.2. Cell cultures and transfection

Plasmids were transiently transfected into human embryonic kidney (HEK)-293 cells by calcium phos-

phate precipitation. For electrophysiology and immunofluorescence, cells were plated on poly-L-lysine (100 µg/ml)-coated glass coverslips prior to transfection. Cells were maintained in minimum essential Eagle's medium supplemented with 10% foetal bovine serum (Invitrogen), 2 mM L-glutamine, 100 U/ml penicillin and 100 µg/ml streptomycin (Invitrogen). Twenty-four hours after transfection, cells were washed with fresh medium and were used 24 h after for further experiments.

### 2.3. Binding experiments

[$^{125}$I]$\alpha$-Bungarotoxin and [$^{3}$H]epibatidine binding assays were performed in phosphate-buffered saline (PBS), as described previously [14], except that GF/C filters (Whatman) were soaked in 0.5% polyethylenimine (PEI, Sigma). Membrane fragments were prepared from transfected cells as described [15] in PBS supplemented with protease inhibitor cocktail tablets (Roche). Water-soluble AChBP expressed in the HEK-293 cells culture media was concentrated in a centrifuge filter device (YM-50, Amicon) followed by a dialysis against PBS for 3 h. [$^{125}$I]$\alpha$-Bungarotoxin and [$^{3}$H]epibatidine binding was determined as described above. In all cases, the $B_{max}$ values of the chimeras were less than the measured $K_D$ values, which exclude ligand depletion. Non-specific binding was determined with either 1 mM L-nicotine or 5 mM of ACh or 5 mM carbamycholine. Protein concentration was determined by the Bradford method.

### 2.4. Sucrose gradient

Membrane fragments were solubilized for 3–4 h in 150 mM NaCl, 5 mM EDTA, 50 mM Tris HCl pH 7.4, 0.02% $NaN_3$, and 1% Triton-X 100. Solubilized chimeric receptors were layered onto 5–30% linear sucrose gradient and centrifuged for 14 h at 37 000 rpm ($\omega^2 t = 7.5 \times 10^{11}$). Fractions of 200 µl were incubated with 5 nM [$^{3}$H]epibatidine for 1 h. Samples were rapidly filtered on three filters soaked in 3% PEI and filters were scintillation-counted. Human $\alpha 4\beta 2$ receptor (10 S) was used as standard.

### 2.5. Electrophysiology

Electrophysiological recordings were performed as described previously [14]. Briefly macroscopic currents were recorded 2–3 days after transfection, using the whole-cell patch-clamp technique [16], with cells at a holding potential −60 mV. Normal external solution contained 140 mM NaCl, 2.8 mM KCl, 2 mM $CaCl_2$, 2 mM $MgCl_2$, 10 mM glucose, and 10 mM HEPES NaOH, pH 7.3. Since 5-$HT_{3A}$ channels are blocked by external $Ca^{2+}$ and $Mg^{2+}$ [17], both ions were suppressed from the external medium just before (and during) ACh applications. Patch pipettes (1–2 MΩ) were filled with a solution containing 140 mM $CsCl_2$, 2 mM MgATP, 10 mM EGTA, and 10 mM HEPES CsOH, pH 7.3. ACh and control solutions were delivered directly to the cell with the aid of a computer-driven system (SF 77A Perfusion fast step, Warner), that ensured a 10–90% solution exchange in 5–10 ms.

### 2.6. Immunofluorescent localization of the chimeras

Transfected HEK-293 cells were fixed in 4% paraformaldehyde in PBS. To label the C-terminal domain, fixed cells were incubated for 2 h with rabbit polyclonal anti-HA antibody (Sigma) diluted 1:100. Fluorescein-conjugated anti-rabbit IgG (diluted 1:1000, Vector) was then applied for 1 h. Intracellular expression of the chimeras was determined by addition of 0.1% Trition X-100 for membrane permeabilization. Glass coverslips were mounted in vectashield mounting medium with a nucleus dye (Dapi, Vector) and immunofluorescence was observed using a Zeiss–Axiophot microscope.

## 3. Results and discussion

*Lymnaea* AChBP was fused linearly either with the mouse cationic serotonin type-3A (5$HT_{3A}$) ion channel or with the human anionic glycine ion channel at the level of pre-M1 (Arg-202) thus yielding AChBP/5$HT_{3A}$ or AChBP/Gly chimeras (Fig. 1A and B). We chose this locus because of the presence of the highly canonical Arg-203 residue that is not conserved in AChBP, but may be crucial for the expression of a full-length receptor (Fig. 1A). Transient transfection of the different cDNAs into HEK-293 cells did not give surface binding sites for either AChBP chimeras as assayed in intact cells with 4.5 nM of the cell-impermeant competitive antag-

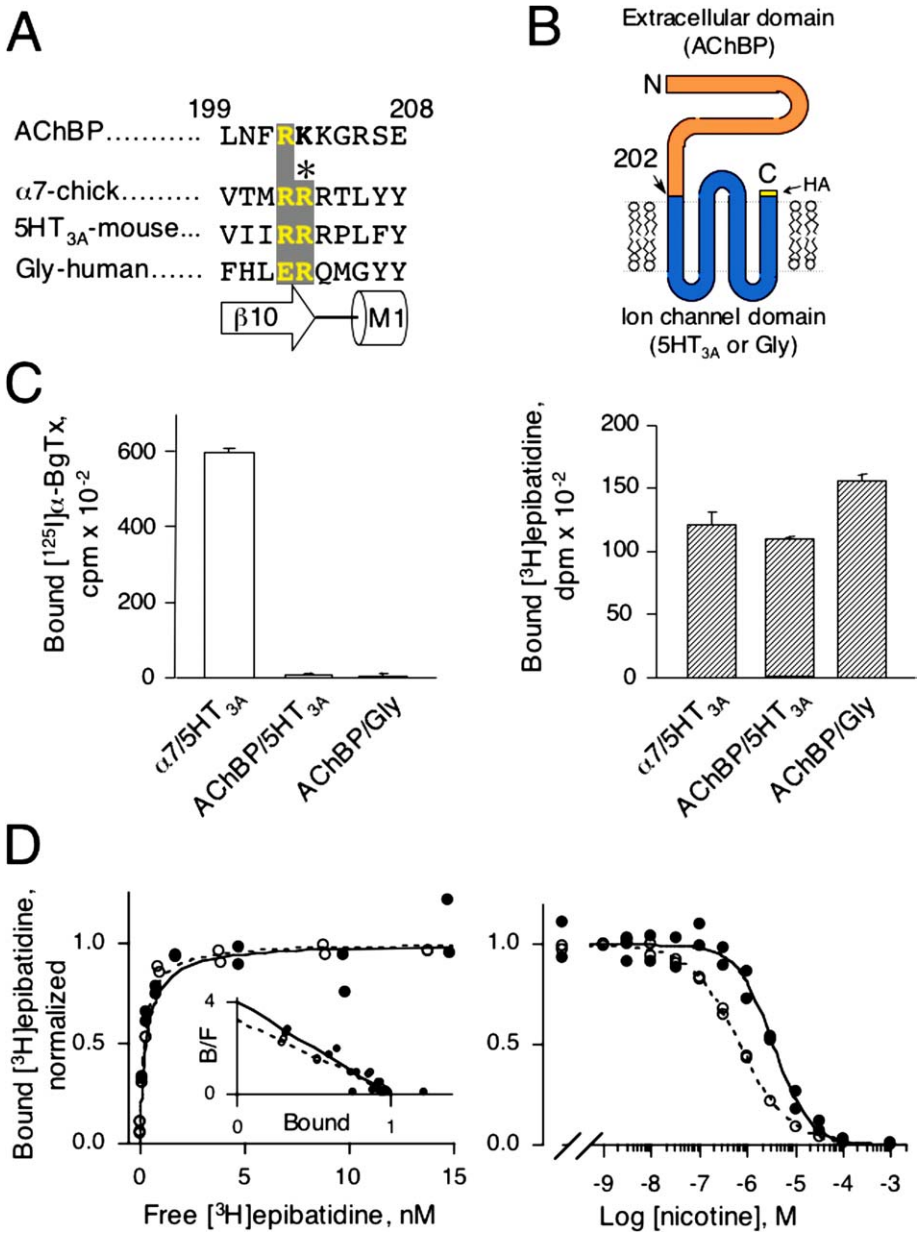


Fig. 1. (**A**) Sequence alignment of *Lymnaea* AChBP, chick $\alpha$7, mouse $5HT_{3A}$, and human Glycine receptors in the pre-M1 region. Numbering refers to the AChBP. Under the sequence alignment is shown the corresponding secondary structures with strand $\beta$10 of AChBP and $\alpha$-helix M1 of the ion channel. (**B**) Cartoon of the predicted topology of a subunit belonging to the LGIC super-family. Here, AChBP (the extracellular domain) is linearly fused after Arg-202 with either $5HT_{3A}$ or glycine ion channel. The human hemagglutinin (HA) epitope is fused to the C-terminal end of the chimera. (**C**) [$^{125}$I]$\alpha$-BgTx (left) and [$^{3}$H]epibatidine (right) binding for the chimeras $\alpha$7/$5HT_{3A}$, AChBP/$5HT_{3A}$ and AChBP/Gly. 4.5 nM [$^{125}$I]$\alpha$-BgTx for 2 h or 5 nM [$^{3}$H]epibatidine for 1 h were added on intact cells expressing chimeras. Samples were filtered and counted. Values $\pm$ SD are specific binding determined by the difference between total binding (without nicotine) and non-specific binding (with 1 mM L-nicotine). (**D**) Representative [$^{3}$H]epibatidine saturation (left) and competition (right) experiments for AChBP/$5HT_{3A}$ chimera (●) and water-soluble AChBP (○). For saturation, non-specific binding was determined with 1 mM L-nicotine and indicated values are specific binding. For competition 2 or 5 nM [$^{3}$H]epibatidine was used for water-soluble AChBP or AChBP/$5HT_{3A}$ chimera, respectively. For both plots, normalized duplicate values of bound [$^{3}$H]epibatidine are shown. Inset: Scatchard representation.

Table 1
Binding parameters of the chimeras

| | [$^3$H]epibatidine binding | | Nicotine binding | | $\alpha$-BgTx binding | |
|---|---|---|---|---|---|---|
| Constructs | $K_D$ (nM) | nH | $K_I$ (nM) | nH | $K$ (nM) | nH |
| Soluble AChBP | $0.20 \pm 0.06$ | $0.90 \pm 0.08$ (3) | $58 \pm 6$ | $0.80 \pm 0.03$ (2) | $4.6 \pm 2.9$[1] | $1.6 \pm 0.01$ (2) |
| Intact cells | | | | | | |
| AChBP/5HT$_{3A}$ | $0.52 \pm 0.27$ | $0.86 \pm 0.16$ (2) | $370 \pm 45$ | $1.00 \pm 0.16$ (2) | ND | |
| AChBP/Gly | $0.25 \pm 0.02^*$ | $0.94 \pm 0.17^*$ (1) | $145 \pm 29^*$ | $0.94 \pm 0.16^*$ (1) | ND | |
| AChBP(ring)/5HT$_{3A}$ | $2.13 \pm 0.32$ | $1.06 \pm 0.03$ (3) | $3680 \pm 750$ | $0.73 \pm 0.03$ (2) | $3500 \pm 1130$[2] | $0.46 \pm 0.07$ (3) |
| | | | | | $20 \pm 49$ [$23 \pm 13$][3] | $0.78 \pm 0.27$ (3) |
| | | | | | $10\,900 \pm 7200$ [$77 \pm 13$][3] | |
| Membrane fragments | | | | | | |
| AChBP(ring)/5HT$_{3A}$ | $14.2 \pm 3.9$ | $0.94 \pm 0.04$ (2) | $14\,800 \pm 1100$ | $1.66 \pm 0.84$ (2) | $173 \pm 78$[2] | $0.38 \pm 0.06$ |
| | | | | | $48 \pm 1$ [$81 \pm 1$][3] | $0.67 \pm 0.01$ (3) |
| | | | | | $> 1\,000\,000$ [$19 \pm 1$][3] | |

ND: not detected since these constructs do not reach the cell surface.

Nicotine binding was measured by equilibrium competition against [$^3$H]epibatidine binding, yielding the apparent $IC_{50}$ from fitting the Hill equation to the data and corrected $K_I$ values were calculated from Cheng–Prussov equation. Values are means ± standard deviation (SD) and the number of determinations is given in parentheses. Asterisks indicate SD of the fitted parameters.

[1] $\alpha$-BgTx binding affinity was measured by competition against initial rate of [$^{125}$I]$\alpha$-BgTx as previously described [15].

[2] $\alpha$-BgTx binding was measured by competition against [$^3$H]epibatidine binding, yielding apparent K as described in [14] from fitting a one-site inhibition model.

[3] For AChBP(ring)/5HT$_{3A}$ chimera a two-site inhibition model is also given according to equation: $\alpha/(1 + (L/K_1)^{nH}) + (1 - \alpha)/(1 + (L/K_2)^{nH})$ where $\alpha$ and $(1 - \alpha)$ are the proportions of high and low affinity sites, respectively (indicated in brackets), $L$ is the concentration $\alpha$-BgTx, nH is the Hill coefficient, and $K_1$ and $K_2$ are the apparent affinity constants for high- and low-affinity sites, respectively.

All constructs were HA tagged to the C-terminal end, except water-soluble AChBP.

onist [$^{125}$I]$\alpha$-bungarotoxin ([$^{125}$I]$\alpha$-BgTx) in conditions where significant [$^{125}$I]$\alpha$-BgTx binding sites were observed with the $\alpha$7/5HT$_{3A}$ chimera fused at the same residue Arg-202 (Fig. 1C, left). Similarly, no intracellular [$^{125}$I]$\alpha$-BgTx binding sites were detected when cells were made permeable with 0.5% (w/v) of saponin (data not shown). However, both chimeric receptors showed equivalent [$^3$H]epibatidine binding, a cell-permeant agonist (Fig. 1C, right). Saturation experiments with [$^3$H]epibatidine revealed that both AChBP chimeras displayed very high-affinity sites for epibatidine ($K_D = 0.52 \pm 0.27$ nM for AChBP/5HT$_{3A}$ and $K_D = 0.25 \pm 0.02$ nM for AChBP/Gly, Table 1 and Fig. 1D) very similar to the affinity of the water-soluble form of AChBP ($K_D = 0.20 \pm 0.06$ nM, see also [18]). The linearity of the Scatchard plot of the binding data to the fused proteins suggests homogeneous population of sites with apparent Hill coefficients close to unity (see Table 1 and Fig. 1D, left inset). Competition experiments revealed a slight decrease of the apparent affinity for nicotine ($K_I = 370 \pm 45$ nM for AChBP/5HT$_{3A}$ and $K_I = 145 \pm 29$ nM for AChBP/Gly) compared to the water-soluble AChBP ($K_I = 58 \pm 6$ nM, Fig. 1D, right; see also [7,11,18]). However, reliable ACh-evoked currents were not detected for either AChBP chimeras using whole-cell patch-clamp, whereas $\alpha$7/5HT$_{3A}$ chimeric receptor displayed significant ACh-evoked currents (Fig. 2D). Since epibatidine crosses the cell membrane, epibatidine binding data suggest that both AChBP/5HT$_{3A}$ and AChBP/Gly sites are produced inside the HEK-293 cells, retained in the ER/Golgi, thus explaining the lack of functionality.

To address whether AChBP chimeras are targeted to the cell surface, we tagged the human hemagglutinin HA epitope to the carboxy terminus of AChBP/5HT$_{3A}$ and AChBP/Gly known to preserve the functionality of the $\alpha$7/5HT$_{3A}$ chimeric receptor [19]. Given the predicted membrane topology of the receptor, the HA epitope is expected to have an extracellular location that can be recognized by extracellular application of anti-HA antibodies when the receptor is

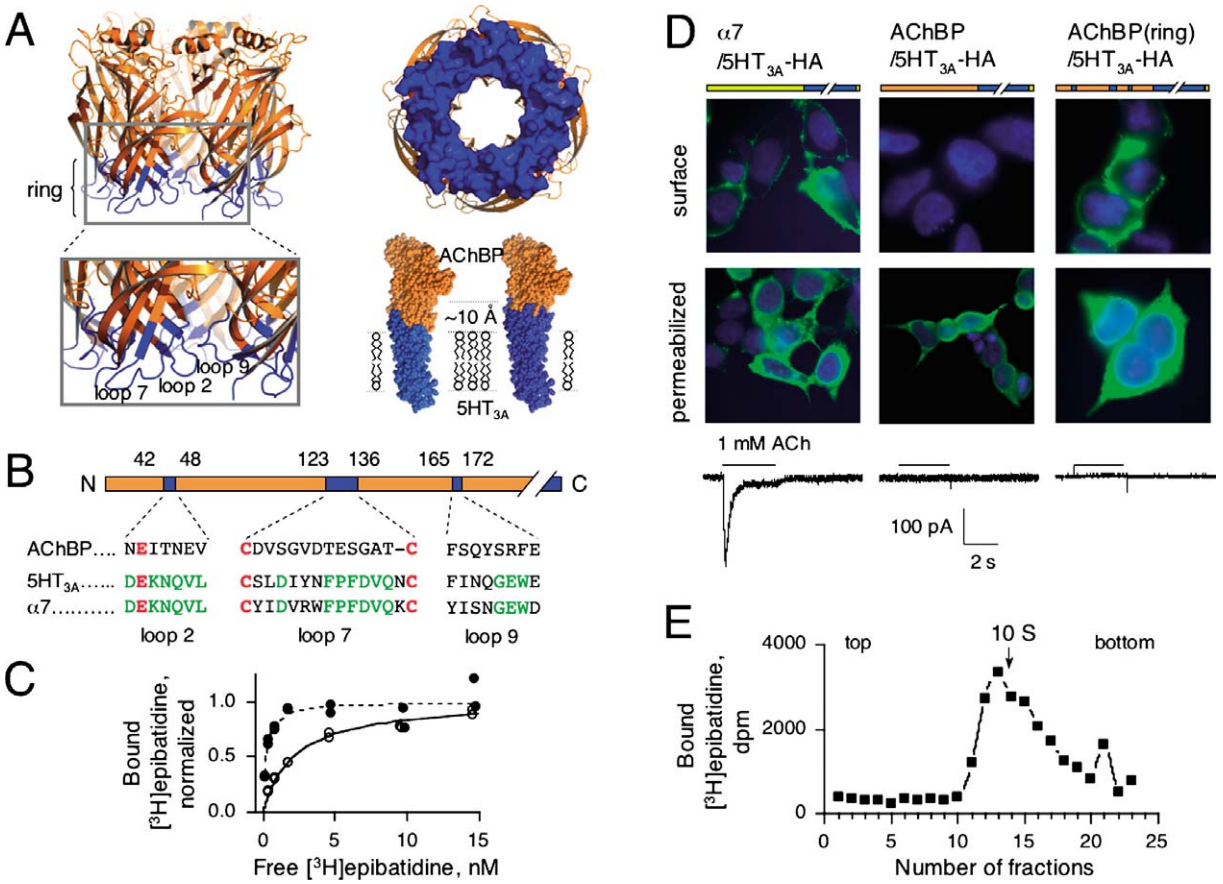


Fig. 2. (**A**) Left, three-dimensional (3D) structure of AChBP (PBD code: 1I9B) [4] with loops 2, 7 and 9 coloured in blue. These loops form a ring of residues located at the membrane side of the 3D structure of AChBP. Right up, view from the channel of the ring. Right down, CPK representation of 3D comparative models of chimeras AChBP/$5HT_{3A}$ and AChBP(ring)$5HT_{3A}$. AChBP and $5HT_{3A}$ residues are coloured in orange and blue, respectively. The ring of $5HT_{3A}$ residues extends 10 Å towards the extracellular domain. (**B**) Linear schematic representation of AChBP (same colour-code as in A). Aligned sequences of loops 2, 7 and 9 are indicated. Canonical residues are shown in red and conserved residues between $\alpha 7$ and $5HT_{3A}$ are indicated in green. (**C**) Representative [$^3$H]epibatidine saturation experiments for AChBP/$5HT_{3A}$ (●) and AChBP(ring)/$5HT_{3A}$ (○) chimeras. Specific normalized duplicate values are shown. (**D**) Immunofluorescence localization of $\alpha 7$/$5HT_{3A}$ (left), AChBP/$5HT_{3A}$ (middle), AChBP(ring)/$5HT_{3A}$ (right). Transfected cells were assayed for cell surface expression (surface) or for the intracellular expression (permeabilized in the presence of 0.1% Triton X-100) of HA-tagged chimeras. Corresponding ACh-evoked currents are indicated under each construct. (**E**) Sucrose gradient sedimentation of AChBP(ring)/$5HT_{3A}$. Each fraction was assayed for [$^3$H]epibatidine binding. Arrow indicates the sedimentation coefficient (10S) of the human $\alpha 4\beta 2$ receptor [20].

inserted on the cell surface (Fig. 1B). Immunofluorescence was clearly visible on the cell surface of intact cells expressing $\alpha 7$/$5HT_{3A}$-HA, but not on those expressing AChBP/$5HT_{3A}$-HA (Fig. 2D 'surface condition') or AChBP/Gly-HA chimeras (not shown). However permeabilized cells showed fluorescence labelling inside the cells (Fig. 2D 'permeabilized condition'). From these results, we concluded that the chimeras AChBP/$5HT_{3A}$-HA and AChBP/Gly-HA did not reach the cell surface, in accordance with the lack of both $\alpha$-BgTx binding sites and of ACh-evoked currents. We therefore reasoned that although high-affinity sites were detected inside the cells expressing the fused proteins, the interface between the binding and the channel domains was not properly formed, thus preventing cell surface expression and channel gating.

Examinations of the crystal structure of the AChBP [5] and of the recent EM structure of the transmembrane domain of the *Torpedo* nAChR [6] suggest

Table 2
[$^3$H]epibatidine binding results for chimeras displaying the different loops combination

| Constructs | loop 2 | loop 7 | loop 9 | dpm/mg[1] | Cell surface[2] |
|---|---|---|---|---|---|
| AChBP | AChBP | AChBP | AChBP | 15 100 ± 1600 (3) | no |
| (loop 2) | $5HT_{3A}$ | AChBP | AChBP | 6000 ± 2000 (4) | no |
| (loop 7) | AChBP | $5HT_{3A}$ | AChBP | 520 ± 270 (4) | no |
| (loop 9) | AChBP | AChBP | $5HT_{3A}$ | 490 ± 90 (3) | no |
| (loops 2+7) | $5HT_{3A}$ | $5HT_{3A}$ | AChBP | 510 ± 200 (4) | no |
| (loops 7+9) | AChBP | $5HT_{3A}$ | $5HT_{3A}$ | 730 ± 120 (4) | no |
| (loops 2+9) | $5HT_{3A}$ | AChBP | $5HT_{3A}$ | 630 ± 60 (4) | no |
| ring | $5HT_{3A}$ | $5HT_{3A}$ | $5HT_{3A}$ | 8800 ± 3600 (4) | yes |
| not transfected | | | | 270 ± 230 (3) | – |

[1] Specific dpm are indicated. Non-specific values were determined in the presence of 1 mM L-nicotine. For comparison between chimeras binding values were normalized to the concentration of proteins (expressed in mg). Values are means ± SD with the number of determination indicated in parentheses.

[2] Cell surface was determined by immunofluorescence experiments on intact cells (see § *Materials and methods*).

that, in the chimeras, the putative membrane side of the AChBP interacts, through still undefined specific interactions, with elements of the transmembrane domain. The crystal structure of the AChBP shows that the putative membrane side of the protein, defined by the location of the C-terminus, is made of three loops (loops 2, 7 and 9, according to nomenclature of [5], Fig. 2A). Aligned sequences revealed that loops 2 (or $\beta$1-$\beta$2 loop: Asn-42 to Val-48, AChBP numbering), 7 (or Cys-loop: Cys-123 to Cys-136) and 9 (or $\beta$8-$\beta$9 loop: Phe-165 to Glu-172) are relatively conserved among the Cys-loop super-family but are not conserved between AChBP and all members of the LGIC (Fig. 2B). Therefore, we hypothesized that restoring homogenous coupling between the two domains would help both the targeting and gating of the chimeric receptor. In the AChBP/$5HT_{3A}$-HA chimera, we substituted residues within these three loops of AChBP with their $5HT_{3A}$ counterparts. This created a 'ring' of $5HT_{3A}$ residues serving as an interface of $\sim$ 10 Å between the AChBP and $5HT_{3A}$ portions of the chimera, as visualized in the atomic structure of AChBP and in our 3D model of the chimera (Fig. 2A). The AChBP(ring)/$5HT_{3A}$-HA chimera showed a four-fold and a ten-fold lower apparent affinity for epibatidine and nicotine, respectively, than its ringless counterparts ($K_D$ epibatidine $= 2.13 \pm 0.32$ nM for AChBP(ring)/$5HT_{3A}$-HA versus $K_D$ epibatidine $= 0.52 \pm 0.27$ nM for AChBP/$5HT_{3A}$-HA, Fig. 2C). Interestingly, contrary to AChBP/$5HT_{3A}$-HA, the ring construct AChBP(ring)/$5HT_{3A}$-HA is targeted to the cell surface as observed by immunofluorescence. Indeed a rim of fluorescence is observed on the surface of intact cells after immuno-staining by anti-HA mAb, as with $\alpha$7/$5HT_{3A}$-HA chimera (Fig. 2D). Although we can not rule out the possibility that the ring chimera binding sites are not completely folded, as suggested by the slight decrease (4- to 10-fold) of the apparent affinity for the agonists epibatidine and nicotine, these findings are more consistent with the conclusion that the ring of $5HT_{3A}$ residues facilitates proper folding of the ligand-binding domain and the channel moiety that is necessary for successful targeting of the receptor to the cell membrane.

To determine if all loops are required for targeting, we generated chimeras in which only one or two loops in AChBP were changed to $5HT_{3A}$ sequence. Chimeras with single loop substitutions of either loop 7 or 9 displayed no significant [$^3$H]epibatidine binding (Table 2). Loop 2 substitution showed detectable [$^3$H]epibatidine binding, despite a lack of surface expression, as assayed by immunofluorescence experiments. For all combinations of two loops no significant [$^3$H]epibatidine binding was detected (Table 2). We verified that the lack of sites was due to impaired protein folding and not to lack of protein expression since metabolic labelling of the proteins with [$^{35}$S]methionine immunoprecipitated with anti-HA mAb yielded bands with the expected molecular weight on reduced SDS-PAGE (data not shown). Hence, only the three-loop substitution displayed cell surface expression, thus suggesting that a synergistic interplay among all three loops is necessary for protein folding and targeting.

We next checked the functionality of the chimera AChBP(ring)/5HT$_{3A}$-HA. No reliable currents were detected either in transfected HEK-293 cells (Fig. 2D) or in injected *Xenopus* oocytes (not shown) in conditions where significant currents were observed with the $\alpha$7/5HT$_{3A}$-HA chimera (Fig. 2D). Removing the HA epitope did not yield functionality for AChBP(ring)/5HT$_{3A}$ (data not shown). To verify that the ring of 5HT$_{3A}$ residues did not prevent function, we generated the homologous ring in the $\alpha$7/5HT$_{3A}$-HA. Since loop 2 is fully conserved between $\alpha$7 and 5HT$_{3A}$, we substituted only loops 7 and 9 (Fig. 2B). Significant ACh-evoked currents were detected in $\alpha$7(ring)/5HT$_{3A}$-HA expressing HEK-293 cells (data not shown). These results thus demonstrate (1) that the AChBP(ring)/5HT$_{3A}$ is not functional, (2) that the ring of 5HT$_{3A}$ residues does not prevent function of the receptor in $\alpha$7(ring)/5HT$_{3A}$ and (3), thus that some elements in the AChBP chimera prevent gating of the 5HT$_{3A}$ ion channel.

Since AChBP(ring)/5HT$_{3A}$-HA is not functional, the possibility exists that unassembled subunits may reach the cell surface without forming functional pentameric receptors. To test this issue, we size fractioned AChBP(ring)/5HT$_{3A}$-HA chimera by sucrose density gradient and showed a sedimentation coefficient of $\sim$ 9.5 S, as expected for a glycosylated pentameric structure [20] (Fig. 2E). Taken together, we conclude that AChBP(ring)/5HT$_{3A}$-HA chimera expressed in HEK-293 cells forms a membrane bound pentameric structure with a central ion pore locked in a closed high-affinity state for epibatidine (in the nanomolar range).

As mentioned above, we report a slight decrease (4- to 10-fold) in agonist affinity between AChBP/5HT$_{3A}$ and AChBP(ring)/5HT$_{3A}$. This small decrease is probably due to the presence of 5HT$_{3A}$ residues that either directly or indirectly modify the ACh-binding sites located $\sim$ 30 Å above the interface. An alternative hypothesis would be a conformation change of the entire receptor that consequently changes allosterically the apparent agonist affinity from a high (D state) to a low (B state) affinity. However, the expected changes for a functional receptor in agonist affinities are comprised between 100- to 10 000-fold [21], not consistent with the 4- to 10-fold decrease we found for both epibatidine and nicotine (Table 1). We thus decided to discriminate between these hypotheses by using a compound known to exhibit higher affinity for the B than for the desensitized D state. Three-finger snake toxins block competitively nicotinic receptors [22] and AChBP [23] by targeting the ACh-binding sites preferentially to the B state of the receptor [24–26]. We therefore determined the affinity of $\alpha$-BgTx for the chimera by measuring on intact cells the displacement of bound [$^3$H]epibatidine by increasing concentrations of $\alpha$-BgTx. Fitting the data to a one-site Hill equation showed very low affinity ($3.5 \pm 1.1$ µM) and a Hill coefficient of $0.46 \pm 0.07$, strongly suggesting a heterogeneous population of sites (Fig. 3A). Fitting the data

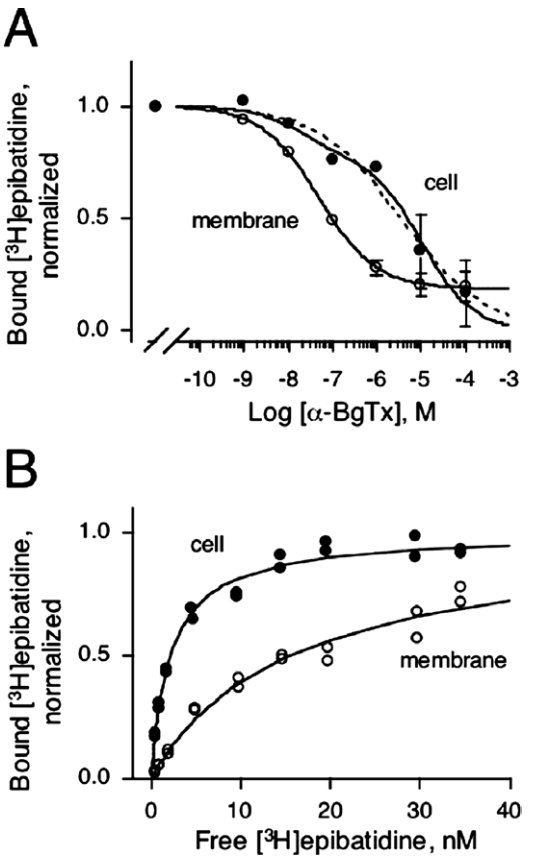


Fig. 3. (**A**) Displacement of 5 nM bound [$^3$H]epibatidine by increasing concentrations of $\alpha$-BgTx on intact cells (●) or on membranes (○) for AChBP(ring)/5HT$_{3A}$. Non-specific binding was determined with either 5 mM ACh or with 5mM carbamylcholine and indicated values are specific binding means ± SD. Dotted and solid lines are fitted curves for one site and two site inhibition models, respectively. (**B**) Representative [$^3$H]epibatidine saturation experiment for AChBP(ring)/5HT$_{3A}$ on intact cells (●) or on membranes (○). Specific normalized duplicate values to $B_{max}$ are shown.

to a two-site Hill equation resulted in approximately 20% of the sites displaying high affinity ($20 \pm 49$ nM) and 80% low affinity for $\alpha$-BgTx ($11 \pm 7$ µM, Table 1). In our conditions, water-soluble AChBP displayed a high affinity for $\alpha$-BgTx ($K_I = 4.6 \pm 2.9$ nM, Table 1), as previously described [7,18]. To verify that this dramatic loss of the apparent affinity for $\alpha$-BgTx was not due to changes in the intrinsic affinity due to the presence of $5HT_{3A}$ residues near the toxin-binding site, we measured [$^{125}$I]$\alpha$-BgTx binding to $\alpha$7(ring)/$5HT_{3A}$-HA chimera expressing cells; significant binding sites were detected at the same level as $\alpha$7/$5HT_{3A}$-HA chimera (data not shown). We thus concluded that the three loops of $5HT_{3A}$ residues do not interfere with toxin binding and that the dramatic apparent loss of toxin affinity for AChBP(ring)/$5HT_{3A}$-HA chimera was mainly due to the shift in the equilibrium between D and B states. Hence, all these results strongly support the following conclusions: (*i*) the presence of the $5HT_{3A}$ ring residues gives rise to an allosteric change of the protein, yet not sufficient to promote a functional receptor; the $\sim$ 20% of high-affinity sites for $\alpha$-BgTx that likely correspond to the B state probably do not allow any experimental detection of currents when ACh is present; (*ii*) most of the chimera molecules are stabilized ($\sim$ 80%) in a low-affinity state for $\alpha$-BgTx (µM range), yet this major fraction represents a high-affinity state for epibatidine (nM range); these sites likely correspond to the desensitized state of LGICs since agonists display high affinity for this state, whereas $\alpha$-BgTx stabilizes preferentially the B state of the receptor [24–26]; (*iii*) the native conformation of AChBP is structurally homologous to the 3-D structure of the desensitized state of the nicotinic receptors [27].

We then tried to shift the equilibrium towards the B state by modifying the chimera itself or the environment.

First, we mutated Arg-11, Arg-148 and Asp-149 to the homologous $\alpha$7 residue (R11V, R148W and E149S) in AChBP because, as viewed on the crystal structure [5], these residues form potential salt bridges within or between neighbouring subunits. Our hypothesis was that these salt bridges located at the subunit interfaces would stabilize the D state and the disruption of these strong interactions would favour the resting state. However, the triple mutant in AChBP(ring)/$5HT_{3A}$-HA did not yield any detectable [$^3$H]epibatidine binding (not shown). Furthermore, we confirmed by immunofluorescence that the triple mutant did not reach significantly the cell surface and likely impaired the folding of the protein.

Second, we prepared membrane fragments from AChBP(ring)/$5HT_{3A}$-HA expressing cells and determined the apparent affinity for both epibatidine and $\alpha$-BgTx. When binding assays were performed in membrane preparations the apparent affinity for epibatidine and nicotine decreased by $\sim$ 5-fold, whereas the proportion of $\alpha$-BgTx high-affinity sites increased up to 80% ($IC_{50} = 48 \pm 1$ nM, Fig. 3A and B, Table 1). These results suggest that, after in vitro preparation of the membrane bound receptor, the chimera undergoes discrete allosteric transitions. We conclude that when the receptor is expressed at the cell surface of HEK-293, it is stabilized mainly in a conformation close to the D state of LGICs, but that during membrane preparation the elements that stabilized the receptor are partially or totally lost, thus shifting a new equilibrium towards the B state. Further investigations are needed to identify such elements; one likely hypothesis would be the presence of regulatory proteins such as protein kinase A known to desensitize the $5HT_3$ receptor through phosphorylation most probably in the cytoplasmic loops [28]. This hypothesis is consistent with the fact that water-soluble AChBP, which lacks an ion channel, binds toxins in the nanomolar range in a state different from the state that binds agonists [18].

During the preparation of the present manuscript, Bouzat et al. [29] reported the fusion of *Lymnaea* AChBP with the rat $5HT_{3A}$ ion channel into a functional structure. The fusion site is located exactly at the same locus as the present report (at the level of Arg-202). They mutated also the three loops at the putative membrane side of AChBP to human $5HT_3$ residues; loop 2: (Asn-42 to Glu-47), loop 7: (Cys-123 to Cys-136) and loop 9: (Phe-165 to Glu-172). Their AChBP(ring)/$5HT_{3A}$ transfected in Bosc-23 cells (a highly transfectable modified version of HEK-293 cells) is targeted to the cell membrane, binds $\alpha$-BgTx and is functional. This finding to some extent contrasts with our data, since we failed to record reliable currents with our chimera. Yet, two differences can explain the contrasted results. First, the so-called 'ring' differs by two point mutations, Val48Leu and Ile166Met. These differences while minor may explain the lack of functionality. Second, Bouzat et al.

[29] used the rat $5HT_{3A}$ ion channel, whereas we used the mouse one. Sequence alignment of the two species revealed major differences in the cytoplasmic M3-M4 loop. A six-amino acid deletion and point mutations are present in the rat sequence. Six Ser-phosphorylation sites are predicted in this region for the rat sequence, whereas only two are predicted for the mouse sequence. These differences in the phosphorylation pattern might modify the function of the receptor as observed for the mouse $5HT_3$ receptor [30]. If that is the case, the pattern of phosphorylations of our chimera probably prevents the receptor from converting substantially into the resting state in intact cells. However, we showed that discrete allosteric transition is possible after membrane preparation for AChBP(ring)/$5HT_{3A}$ and thus that part of AChBP has preserved the structural elements that are necessary for allosteric transitions in agreement with Bouzat et al. [29].

In conclusion, we show in this paper that linear fusion of AChBP with either the cationic $5HT_{3A}$ ion channel or the anionic glycine ion channel forms high-affinity sites for epibatidine. These results suggest that the AChBP module recognizes any ion channel modules of the Cys-loop super-family, extending the previous observation [4] of autonomous folding of the two main receptor domains: the ligand-binding and channel domains. This finding is of interest since AChBP has probably evolved without the constraint of an ion channel and thus loops 2, 7 and 9 have diverged from their ancestral receptor. Replacement of the AChBP ring (loops 2, 7 and 9) by the $5HT_{3A}$ counterparts restores a three-dimensional homogeneous coupling between the extracellular domain and the ion channel necessary for targeting to the cell surface. Finally, we showed that the chimeric ring receptor is able to mediate discrete allosteric transitions (i.e. shift the equilibrium in favour to B) that consequently decrease the apparent affinity for both epibatidine and nicotine. Hence, part of AChBP conserved during evolution the capacity to make allosteric isomerizations.

## Acknowledgements

This work was supported by the ‘Collège de France’, the ‘Association pour la recherche contre le cancer’, the ‘Commission of the European Communities’ (CEC contracts Nos. 2002-00258 and 2000-00318), and the ‘Association française contre les myopathies’. We thank Drs J. Neyton for experiments with oocytes, P.J. Corringer for discussion, B. Molles for critical reading of the manuscript and H. Betz for providing the human glycine receptor clone. A.T. is the recipient of a fellowship from the ‘Association française contre les myopathies’.

## References

[1] P.-J. Corringer, N. Le Novère, J.-P. Changeux, Nicotinic receptors at the amino acid level, Annu. Rev. Pharmacol. 40 (2000) 431–458.

[2] A. Karlin, Emerging structure of the nicotinic acetylcholine receptors, Nat. Rev. Neurosci. 3 (2002) 102–114.

[3] J.-P. Changeux, S.J. Edelstein, Allosteric receptors after 30 years, Neuron 21 (1998) 959–980.

[4] J.-L. Eiselé, S. Bertrand, J.-L. Galzi, A. Devillers-Thiéry, J.-P. Changeux, D. Bertrand, Chimeric nicotinic serotonergic receptor combines distinct ligand-binding and channel specificities, Nature 366 (1993) 479–483.

[5] K. Brejc, W.J. van Dijk, R.V. Klaassen, M. Schuurmans, J. van der Oost, A.B. Smit, T.K. Sixma, Crystal structure of an ACh-binding protein reveals the ligand-binding domain of nicotinic receptors, Nature 411 (2001) 269–276.

[6] A. Miyazawa, Y. Fujiyoshi, N. Unwin, Structure and gating mechanism of the acetylcholine receptor pore, Nature 423 (2003) 949–955.

[7] A.B. Smit, N.I. Syed, D. Schaap, J. van Minnen, J. Klumperman, K.S. Kits, H. Lodder, R.C. van der Schors, R. van Elk, B. Sorgedrager, K. Brejc, T.K. Sixma, W.P.M. Geraerts, A glia-derived acetylcholine-binding protein that modulates synaptic transmission, Nature 411 (2001) 261–268.

[8] N. Le Novère, T. Grutter, J.-P. Changeux, Models of the extracellular domain of the nicotinic receptors and of agonist- and $Ca^{2+}$-binding sites, Proc. Natl Acad. Sci. USA 99 (2002) 3210–3215.

[9] M. Ernst, D. Brauchart, S. Boresch, W. Sieghart, Comparative modeling of GABA(A) receptors: Limits, insights, future developments, Neuroscience 119 (2003) 933–943.

[10] D.C. Reeves, M.R.F. Sayed, P.L. Chau, K.L. Price, S.C.R. Lummis, Prediction of $5HT_3$ receptor agonist-binding residues using homology modeling, Biophys. J. 84 (2003) 2338–2344.

[11] P.H.N. Celie, S.E. van Rossum-Fikkert, W.J. van Dijk, K. Brejc, A.B. Smit, T.K. Sixma, Nicotine and carbamylcholine binding to nicotinic acetylcholine receptors as studied in AChBP crystal structures, Neuron 41 (2004) 907–914.

[12] T.L. Kash, A. Jenkins, J.C. Kelley, J.R. Trudell, N.L. Harrison, Coupling of agonist binding to channel gating in the GABA(A) receptor, Nature 421 (2003) 272–275.

[13] T.L. Kash, M.J.F. Dizon, J.R. Trudell, N.L. Harrison, Charged residues in the $\beta 2$ subunit involved in GABA(A) receptor activation, J. Biol. Chem. 279 (2004) 4887–4893.
[14] T. Grutter, L. Prado de Carvalho, N. Le Novère, P.-J. Corringer, S. Edelstein, J.-P. Changeux, An H-bond between two residues from different loops of the acetylcholine binding site contributes to the activation mechanism of nicotinic receptors, EMBO J. 22 (2003) 1990–2003.
[15] P.J. Corringer, J.-L. Galzi, J.-L. Eiselé, S. Bertrand, J.-P. Changeux, D. Bertrand, Identification of a new component of the agonist binding-site of the nicotinic $\alpha 7$ homooligomeric receptor, J. Biol. Chem. 270 (1995) 11749–11752.
[16] O.P. Hamill, A. Marty, E. Neher, B. Sakmann, F.J. Sigworth, Improved patch-clamp techniques for high-resolution current recording from cells and cell-free membrane patches, Pflugers Arch. 391 (1981) 85–100.
[17] A.V. Maricq, A.S. Peterson, A.J. Brake, R.M. Myers, D. Julius, Primary structure and functional expression of the $5HT_3$ receptor, a serotonin-gated ion channel, Science 254 (1991) 432–437.
[18] S.B. Hansen, Z. Radic, T.T. Talley, B.E. Molles, T. Deerinck, I. Tsigelny, P. Taylor, Tryptophan fluorescence reveals conformational changes in the acetylcholine binding protein, J. Biol. Chem. 277 (2002) 41299–41302.
[19] S. Rakhilin, R.C. Drisdel, D. Sagher, D.S. McGehee, Y. Vallejo, W.N. Green, Alpha-bungarotoxin receptors contain $\alpha 7$ subunits in two different disulfide-bonded conformations, J. Cell. Biol. 146 (1999) 203–217.
[20] Y. Zhou, M.E. Nelson, A. Kuryatov, C. Choi, J. Cooper, J. Lindstrom, Human $\alpha 4\beta 2$ acetylcholine receptors formed from linked subunits, J. Neurosci. 23 (2003) 9004–9015.
[21] T. Heidmann, J. Bernhardt, E. Neumann, J.-P. Changeux, Rapid kinetics of agonist binding and permeability response analyzed in parallel on acetylcholine-receptor rich membranes from *Torpedo marmorata*, Biochemistry 22 (1983) 5452–5459.
[22] C. Fruchart-Gaillard, B. Gilquin, S. Antil-Delbeke, N. Le Novère, T. Tamiya, P.-J. Corringer, J.-P. Changeux, A. Menez, D. Servent, Experimentally based model of a complex between a snake toxin and the $\alpha 7$ nicotinic receptor, Proc. Natl Acad. Sci. USA 99 (2002) 3216–3221.
[23] M. Harel, R. Kasher, A. Nicolas, J.M. Guss, M. Balass, M. Fridkin, A.B. Smit, K. Brejc, T.K. Sixma, E. Katchalski-Katzir, J.L. Sussman, S. Fuchs, The binding site of acetylcholine receptor as visualized in the X-ray structure of a complex between $\alpha$-bungarotoxin and a mimotope peptide, Neuron 32 (2001) 265–275.
[24] D. Bertrand, A. Devillers-Thiéry, F. Revah, J.-L. Galzi, N. Hussy, C. Mulle, S. Bertrand, M. Ballivet, J.-P. Changeux, Unconventional pharmacology of a neuronal nicotinic receptor mutated in the channel domain, Proc. Natl Acad. Sci. USA 89 (1992) 1261–1265.
[25] R.E. Middleton, N.P. Strnad, J.B. Cohen, Photoaffinity labeling the *Torpedo* nicotinic acetylcholine receptor with [$^3$H]tetracaine, a non desensitizing noncompetitive antagonist, Mol. Pharmacol. 56 (1999) 290–299.
[26] M.A. Moore, M.P. McCarthy, Snake-venom toxins, unlike smaller antagonists, appear to stabilize a resting state conformation of the nicotinic acetylcholine-receptor, BBA – Biomembranes 1235 (1995) 336–342.
[27] T. Grutter, J.-P. Changeux, Nicotinic receptors in wonderland, Trends Biochem. Sci. 26 (2001) 459–463.
[28] J.-L. Yakel, M.B. Jackson, $5HT_3$ receptors mediate rapid responses in cultured hippocampus and a clonal cell-line, Neuron 1 (1988) 615–621.
[29] C. Bouzat, F. Gumilar, G. Spitzmaul, H.L. Wang, D. Rayes, S.B. Hansen, P. Taylor, S.M. Sine, Coupling of agonist binding to channel gating in an ACh-binding protein linked to an ion channel, Nature 430 (2004) 896–900.
[30] S. Jones, J.-L. Yakel, Casein kinase ii (protein kinase CK2) regulates serotonin $5HT_3$ receptor channel function in NG108-15 cells, Neuroscience 119 (2003) 629–634.